ACS chemical biology

ARTICLE

Activating B Cell Signaling with Defined Multivalent Ligands

Erik B. Puffer[†], Jason K. Pontrello[‡], Jessica J. Hollenbeck[†], John A. Kink[§], and Laura L. Kiessling[†,‡,*]

[†]Department of Biochemistry, [‡]Department of Chemistry, University of Wisconsin–Madison, Madison, Wisconsin 53706, and [§]Quintessence Biosciences, Inc., 505 South Rosa Road, Madison, Wisconsin 53719

ABSTRACT Depending on the stimuli they encounter, B lymphocytes engage in signaling events that lead to immunity or tolerance. Both responses are mediated through antigen interactions with the B cell antigen receptor (BCR). Antigen valency is thought to be an important parameter in B cell signaling, but systematic studies are lacking. To explore this issue, we synthesized multivalent ligands of defined valencies using the ring-opening metathesis polymerization (ROMP). When mice are injected with multivalent antigens generated by ROMP, only those of high valencies elicit antibody production. These results indicate that ligands synthesized by ROMP can activate immune responses *in vivo*. All of the multivalent antigens tested activate signaling through the BCR. The ability of antigens to cluster the BCR, promote its localization to membrane microdomains, and augment intracellular Ca^{2+} concentration increases as a function of antigen valency. In contrast, no differences in BCR internalization were detected. Our results indicate that differences in the antigenicity of BCR ligands are related to their ability to elicit increases in intracellular Ca^{2+} concentration. Finally, we observed that unligated BCRs cluster with BCRs engaged by multivalent ligands, a result that suggests that signals mediated by the BCR are amplified through receptor arrays. Our data suggest a link between the mechanisms underlying signal initiation by receptors that must respond with high sensitivity.

*Corresponding author, kiessling@chem.wisc.edu.

Received for review December 21, 2006 and accepted February 12, 2007.

Published online April 13, 2007

10.1021/cb600489g CCC: $37.00

With the advent of powerful methods to synthesize compounds that bind multiple copies of receptors, new questions regarding the role of cell surface receptor organization can be probed (*1–3*). Ligand-promoted changes in receptor organization are often critical for activating signaling (*4, 5*). Evidence is emerging that output responses can depend on cell surface receptor location and organization. Defined multivalent ligands can be used to investigate how these factors influence output responses (*1, 2*). Utilizing multivalent ligands generated by the ring-opening metathesis polymerization (ROMP), we have demonstrated previously that ligand valency can influence receptor clustering and signal output (*6–8*). These investigations underscore the utility of synthetic multivalent ligands as mechanistic probes of receptor clustering in cell signaling. They also illustrate the efficacy of these ligands as tools for controlling cellular responses.

The immune system depends on multivalent interactions. For example, B cell activation triggered by multivalent antigens can result in clonal expansion and antibody production. Alternatively, antigen signals can also lead to quiescence or apoptosis (*9*). Antigen signals are transmitted *via* the B cell antigen receptor (BCR), a multiprotein complex on the B cell surface that functions to direct antigen-specific responses (*10*). Indeed, this receptor initiates signaling events leading to both immunity and tolerance (*9, 11*). A number of features of the antigen are thought to influence signaling pathways, including its functional affinity (avidity), dose, and valency. Exploring the effects of antigen structure on signal output can illuminate the features responsible for signal transmission and lead to new strategies to control immune responses.

A variety of methods are being used to elucidate the effect of antigen structure on output responses (*12*). The most common approach is to use antibodies to exam-

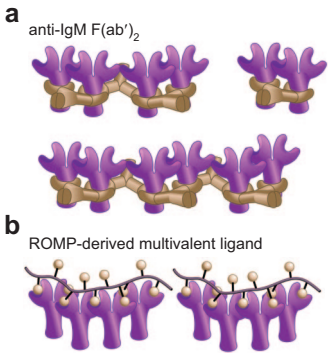

Figure 1. Proposed mechanisms of binding for F(ab′)$_2$ anti-IgM and ROMP-derived multivalent ligand. a) F(ab′)$_2$ anti-IgM μ-chain binds the invariable region of the transfected DNP-specific BCR of the A20/2J HL$_{TNP}$ cell line. In this model, one antibody can engage two BCRs, forming BCR–antibody complexes that vary widely in stoichiometry. b) ROMP-derived multivalent ligands of high valency engage multiple BCRs simultaneously.

ine the role of BCR clustering in immune signaling. These divalent reagents can form noncovalently cross-linked complexes with the divalent BCR, thereby obscuring the role of antigen valency (Figure 1). A related approach uses molecular assemblies composed of biotinylated F(ab′) fragments and tetrameric avidin, termed pseudoantigens (*13*). Activation is greater when cells are stimulated with higher order pseudoantigen assemblies, but the valency of the complexes is not well characterized. Moreover, BCR responses to pseudoantigens can differ from those induced by polyvalent antigens. For example, coreceptors on the cell surface can modulate BCR-mediated signals; however, the use of antibodies to cluster the BCR can interfere with coreceptor function (*14*). Chemical synthesis can be used to assemble multivalent antigens that overcome these drawbacks.

Some studies investigating the role of the BCR employ proteins as the scaffold upon which antigenic epitopes are presented (*15, 16*). With a protein scaffold, antigen valency has been varied by altering the average number of epitopes appended. This approach, however, simultaneously alters antigen density. When the antigen density is altered, the mechanism(s) by which a multivalent ligand acts can also be changed (*17*), thereby complicating analysis. Because the dimensions of the protein scaffold are invariant, investigations with protein ligands of this type cannot reveal the role of receptor clustering.

Chemical synthesis provides the means to generate multivalent ligands that serve as antigens and vary systematically in structure. Polymer functionalization reactions have been used to generate multivalent ligands based on dextran, ficoll, or polyacrylamide derivatives. Studies by others (*18–22*) revealed that polymeric ligands can elicit the production of antibodies in mice. The conclusion of these studies was that a critical number of BCRs (≥20) must be engaged to elicit B cell activation. These studies are an elegant example of exploring how antigen features influence immune signaling. Still, the only response measured, antibody production, involves many different steps. Innovations in chemical synthesis provide the means to generate much more defined antigens, and advances in signal transduction have provided new tools to examine B cell signaling. By combining these developments, we sought to correlate the *in vivo* activities of multivalent antigens with their influence on BCR localization and signal transduction. These studies provide new insight into how antigen valency can be used to control immune responses.

RESULTS AND DISCUSSION

Synthesis of Multivalent Antigens Using ROMP. Typical polymerization methods used to synthesize polyvalent ligands afford highly heterogeneous populations. B cell responses depend on antigen dose, and antigens of different valencies might have different effects on BCR signaling. Accordingly, routes to synthetic antigens of defined valencies are needed. To this end, we applied ROMP to synthesize multivalent antigens. The kinetic parameters of select ruthenium carbene-initiated ROMP reactions can facilitate the synthesis of biologically active polymers of defined molecular mass and narrow polydispersities (*23–28*). By variation of the monomer to initiator (M:I) ratio, multivalent ligands of defined average length (M_n) and low polydispersity indices (PDI) can be generated. The utility of ROMP for generating compounds to investigate and manipulate various signaling pathways has been demonstrated (*6, 7, 29–36*). Here, we employed ROMP under optimized polymerization conditions with a recently reported ruthenium carbene metathesis initiator (*23, 37*). This synthetic method provides multivalent antigens of defined length and hapten substitution to investigate the effect of antigen valency on BCR signaling.

The defined multivalent antigens were generated using a postpolymerization modification strategy (*35, 38*). With this synthetic approach, a polymer backbone is assembled to which antigenic epitopes can be attached.

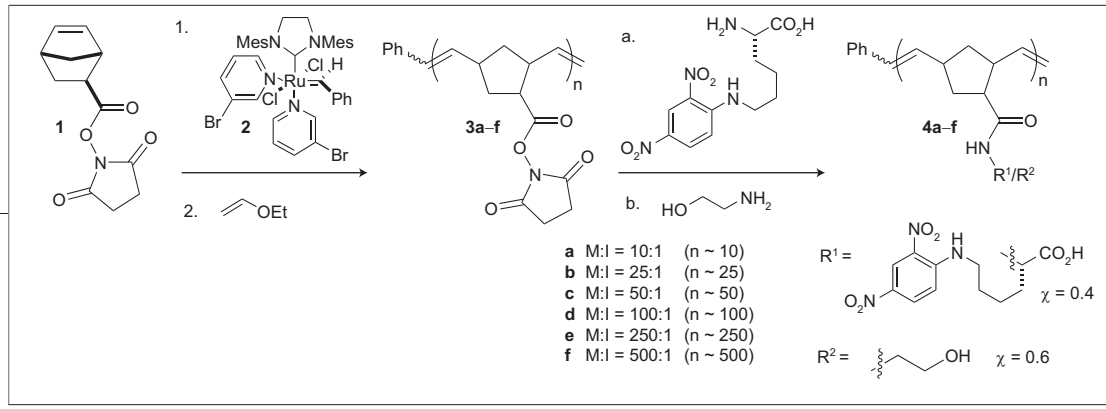

Scheme 1. Route used to assemble multivalent DNP antigens that vary in valency using ROMP.

This synthetic approach is especially valuable for biological studies because a single reaction can afford a variety of substituted polymers with identical lengths and PDI values. To implement this approach, we needed to synthesize polymers bearing a group that can undergo rapid and efficient reaction to append the desired antigenic moieties; this group must also be stable to the polymerization conditions. We used monomers bearing succinimidyl ester groups (**3a**–**f**; Scheme 1), which we had shown can be polymerized using ruthenium carbene initiators to afford amine-reactive polymers. The reactions were conducted using a ruthenium carbene that affords polymers with very narrow polydispersities (PDIs ranging from 1.05 to 1.10) (*23, 34*). We employed this initiator at low temperature (−20 °C) as these conditions afforded the lowest PDI values (*25, 26, 37*). In contrast to results obtained with commercially available ruthenium carbene catalysts, we observed complete consumption of the monomer even at M:I ratios of 1000:1. In addition, the average polymer length (M_n), as determined by comparing the ^{1}H-NMR integration of the signal due to the polymer alkene protons to that due to the terminal phenyl protons, is consistent with that predicted from the M:I ratio. For convenience, we refer to the polymers generated as 10-mer (M:I = 10), 25mer (M:I = 25), *etc*.

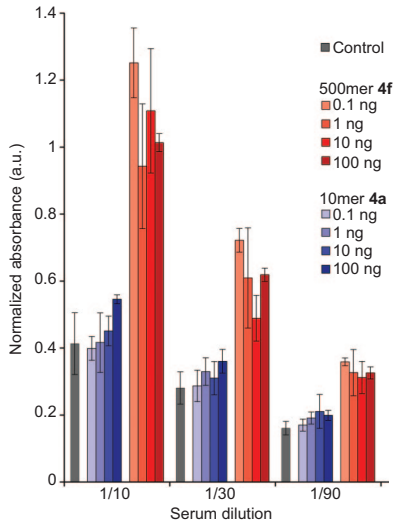

Figure 2. Antibody production in BALB/c mice after injection of synthetic multivalent ligands 4a **and** 4f. **500mer** 4f **induced production of DNP-specific IgM, whereas the 10mer** 4a **did not. The data shown are representative of trends observed for three independent experiments. Error bars depict variation between three mice injected with the same concentration of polymer for a single experiment.**

The antigen that we appended, the 2,4-dinitrophenyl (DNP) group, was selected for two reasons. First, a cell line capable of recognizing and internalizing DNP-substituted antigens has been reported (*16*). Second, DNP-substituted polymers can readily be generated from DNP-lysine; the α-amino group can undergo reaction with the succinimidyl ester-substituted polymers to generate the target multivalent antigens (Scheme 1). Because the DNP group is relatively nonpolar, we sought to enhance the aqueous solubility of the antigen-bearing polymers by substituting only a portion of the available activated ester groups with this moiety. The remaining succinimidyl esters were converted to neutral functionality by the addition of excess ethanolamine to afford antigens **4a**–**f**. The mole fraction (χ) of DNP ligand substituted was determined by comparing the integration of the ^{1}H-NMR signals from the aromatic DNP protons to that of the polymer alkene protons. This analysis indicated that the mole fraction of DNP incorporated was similar for polymers of varying valencies (10mer **4a**, 25mer **4b**, 50mer **4c**, 100mer **4d**, 250mer **4e**, and 500mer **4f**). Specifically, when 0.1 equiv of DNP lysine was used relative to polymer succinimidyl ester, a χ of 0.08–0.10 was obtained; 0.4 equiv of DNP lysine afforded a χ of 0.37–0.40, and 1.0 equiv of DNP lysine gave a χ of 0.80–0.90. As polymers with different mole fractions of DNP had similar activities (data not shown), we focused our investigations on the multivalent antigens generated from 0.4 equiv of DNP lysine relative to succinimidyl ester groups.

Antibody Production Is Influenced by Antigen Valency. *Ligands Generated by ROMP Can Be Used* in Vivo. To evaluate the *in vivo* activity of antigens generated by ROMP, we tested their ability to elicit anti-DNP antibody production in mice. We compared the effects of low and high valency ligands by injecting either the 10mer **4a** or the 500mer **4f** into BALB/c mice. There are no reports describing the effects of polymers of this type *in vivo*. Importantly for these investigations, they had no obvious toxicity. No increase in mortality in polymer-treated mice was observed nor were obvious behavioral changes. These results indicate that polymers of this type can be used for *in vivo* applications.

After 6–15 d, serum IgM concentrations of antibodies specific to the dinitrophenyl hapten were assessed using an enzyme-linked immunosorbent assay (ELISA). Animals treated with the highest valency ligand, 500mer **4f,** exhibited DNP-specific IgM levels significantly higher than that of buffer-treated control animals (Figure 2). This increase was observed for all concentrations of

500mer; immunization with 0.1, 1, 10, or 100 ng of **4f** afforded elevated levels of DNP-binding IgM. Conversely, the lowest valency ligand (10mer, **4a**) failed to elicit detectable anti-DNP antibody production under any conditions tested (Figure 2). Our results indicate that the multivalent antigens generated by ROMP are capable of eliciting immune responses.

The data indicate that high valency antigens are required to initiate immune responses leading to antibody production; the low valency antigen (10mer) did not. In previous experiments, high valency polymers of other types were shown to promote antibody production (*20, 21, 39*). These results led to the conclusion that polymers with molecular weights >60,000 and extended lengths of 4600 Å can cluster ~20 BCRs, and that this level of clustering is required to elicit antibody production. Although we admire these efforts to relate findings on antibody production to the molecular features of the antigens, our data do not support such models. The antibody-eliciting 500mer **4f** is estimated to be <2000 Å (*40, 41*); therefore, it would not be expected to elicit antibodies, yet it does. Presuming that BCR clustering is the critical step leading to antibody production (*vide infra*), it is not surprising that there would be differences in the apparent length requirements for different scaffolds for antigen presentation. The structural features of a multivalent antigen influence its ability to cluster receptors (*42*). Thus, in addition to its length, the structure of an antigen is critical for its activity. Moreover, our data suggest that the number of BCRs that contribute to signaling cannot be estimated by determining the number of BCRs a ligand can engage.

Antigen Valency Modulates Changes in Intracellular Ca^{2+} Levels. The differing abilities of low (*e.g.*, 10mer) and high (*e.g.*, 500mer) valency antigens to elicit signaling might stem from changes in the adsorption distribution or clearance of the polymers. Alternatively, these differences might result from the polymer's abilities to activate signaling. We therefore tested whether polymer valency influences BCR signaling. One key manifestation of antigen-induced signaling is an increase in intracellular Ca^{2+} concentration ($[Ca^{2+}]_i$). Engagement of the BCR by multivalent antigen results in the phosphorylation of kinases that activate phospholipase γ_2 ($PLC\gamma_2$), which in turn produces inositol triphosphate (IP_3). The presence of this second messenger causes the release of Ca^{2+} from the endoplasmic reticulum stores. The increase in $[Ca^{2+}]_i$ then leads to activation of protein kinase C (PKC), which induces additional signal-transduction pathways (*10*). Thus, examining changes in $[Ca^{2+}]_i$ provides a means to determine whether the observed valency-dependent differences in antibody production *in vivo* correlate with early signaling events in antigen-mediated B cell activation. To determine if the polymers elicit a response, we employed a standard flow cytometry assay that relies on the ratiometric dye indo-1, which changes its emission λ maximum when chelated to Ca^{2+} (*43, 44*).

Multivalent DNP Derivatives Are Required for Signaling. Although it has been generally accepted that signaling through the BCR is initiated by BCR clustering, a recent study suggests that monovalent protein antigens can activate signaling (*45*). To ascertain whether low-molecular-weight, monovalent DNP derivatives elicit signaling, we exposed cells to DNP-Lys. We could not detect signaling (*i.e.*, no change in $[Ca^{2+}]_i$). These data indicate that monovalent DNP derivatives do not activate BCR signaling.

One explanation for the inability of low valency antigens to elicit antibodies *in vivo* is that they are unable to activate BCR signaling. When A20/2J HL_{TNP} cells were exposed to the multivalent antigens, a sharp increase in $[Ca^{2+}]_i$ was observed (Figure 3). These data indicate that all of the multivalent ligands generated by ROMP, even the low valency antigens, elicit signaling. To determine whether signaling arises from specific engagement of the BCR, we tested the activity of our most active compound, 500mer **4f**, on the A20 cell line. Because A20 cells do not display a DNP-specific BCR, they should not respond to multivalent antigen. As expected, exposure of these cells to DNP-substituted multivalent ligands did not elicit calcium flux (Figure 3, panel a inset). This result indicates that the increases in intracellular $[Ca^{2+}]$ induced by the multivalent ligands occur only in cells that display a BCR with the proper specificity.

To ascertain whether these ligands function *via* multivalent binding, we tested signal output as a function of antigen concentration. Ligands that act through multivalent binding exhibit a characteristic relationship between ligand concentration and activity. Specifically, activity initially increases with increasing ligand concentration, because the addition of more ligand results in the clustering of more receptors. When the multivalent ligand concentration is very high, however, the receptors become less clustered because complexes between individual multivalent ligands and single receptors can

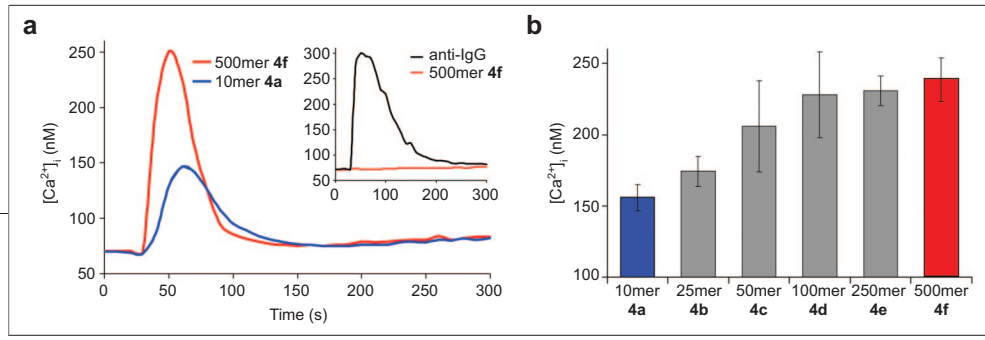

Figure 3. Changes in $[Ca^{2+}]_i$ induced by multivalent ligands. a) Raw calcium flux kinetics profiles for A20/2J HL_{TNP} cells treated with ROMP-derived DNP-substituted 10mer 4a and 500mer 4f. (inset) A20 cells treated with anti-IgG $F(ab')_2$ and ROMP-derived DNP-substituted 500mer 4f. b) Statistical analysis of the peak increase in $[Ca^{2+}]_i$ elicited by multivalent ligands 10mer 4a, 25mer 4b, 50mer 4c, 100mer 4d, 250mer 4e, and 500mer 4f at their most effective concentration (5 μM DNP). These data are the average of $n \geq 3$ on a given day and are representative of a minimum of three independent experiments.

form. If signaling depends on multivalent binding, very high multivalent ligand concentrations will result in a decrease in signal magnitude (*46–48*). To test for this relationship, a concentration curve was determined for each multivalent antigen. All antigens afforded a curve that increased as a function of polymer concentration, peaked at a specific multivalent ligand concentration, and then decreased at high concentrations (Figure 4). This pattern of activity indicates that the BCR response to these antigens depends on multivalent binding.

Intracellular Ca^{2+} Levels Increase with Antigen Valency. Analysis of the concentration curves for antigens of different valencies provides insight into the relationship between antigen valency, antigen dose, and BCR signaling. Regardless of the valency of the antigens, the DNP concentration of each that gives rise to the largest effect corresponds to 5 μM. To compare antigen strength, we performed statistical analysis on the peak fluorescence emission ratio for several replicates ($n \geq 3$) of cells treated with each of the multivalent ligands (5 μM DNP). These data indicate that the magnitude of the Ca^{2+} flux increases as antigen valency (polymer length) increases. At 5 μM DNP, the 500mer affords a larger increase in $[Ca^{2+}]_i$ than does the 10mer (Figure 3, panel b). Differences in the requisite antigen dose required to elicit the maximal signal were also apparent. Maximal signals for the 500mer were obtained at 100-fold lower concentration than those required for the 10mer (100 nM *vs* 1.4 μM). Still, the maximum signal for the 10mer never approaches that of the 500mer. These data underscore the interdependence of antigen valency, antigen dose, and BCR signal output (*9, 11, 49*).

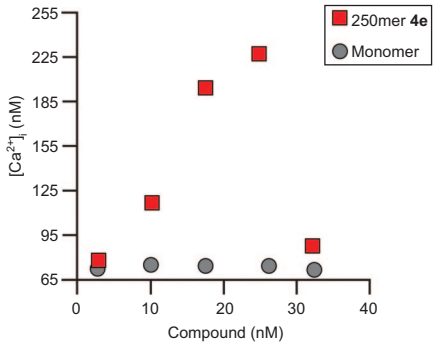

Figure 4. Profile of multivalent ligand-induced calcium influx at various concentrations of multivalent ligand or monomer. Monomeric DNP-lysine does not induce calcium flux at any concentration tested. The profile seen for 250mer 4e is typical for signaling activated by multivalent ligand-induced receptor clustering. At high concentrations of multivalent ligand, signal induction is abolished as the number of receptors bound to each polymer molecule decreases.

The data on antibody production suggest a relationship between the valency of a compound, its ability to elicit antibody production, and its ability to cause large changes in $[Ca^{2+}]_i$. It has been shown that the differences in $[Ca^{2+}]_i$ can influence gene expression in B cells. For example, a large transient release in intracellular $[Ca^{2+}]$ results in activation of the transcriptional regulators nuclear factor κ B (NF-κB) and nuclear factor of activated T cells (NFAT), but a low sustained increase in intracellular $[Ca^{2+}]$ results in nuclear factor of activated T cell activation (*50*). Thus, the degree of calcium flux, which our data indicate can be dictated by antigen valency, might be used to manipulate BCR responses. Our data suggest that calcium signals generated by higher valency antigens give rise to downstream signaling events that reach the threshold for gene expression changes necessary for antibody production, while calcium signals generated by lower valency antigens do not. Evidence exists that antigens unable to achieve the threshold for function-related gene expression give rise to signals for quiescence or apoptosis (*9*). These results are consistent with studies in which low valency antigens can induce tolerance (*22, 51–54*) (reviewed in ref 55). The ability to control antigen valency *via* modern polymerization methods (*56–58*) provides a means to synthesize materials that elicit immunity or tolerance.

Signaling Differences Do Not Arise from Differences in BCR Internalization. The relationship between BCR signaling and internalization is controversial (*59*). It has been suggested that more robust signals may result from ligands that are internalized less effectively (*60*). We therefore tested the different valency ligands to determine whether their abilities to promote BCR internalization might differ. To this end, we compared the extent of BCR internalization in the presence of the 10mer **4a** and the 500mer **4f** (Figure 5). Multivalent ligands were incubated with the cells at either 4 or 37 °C, and a Cy5-labeled F(ab') fragment with specificity for the BCR (anti-IgM) was used to label the remaining surface BCR. As a positive control for internalization, A20/2J HL_{TNP} cells were exposed to DNP-substituted bovine serum albu-

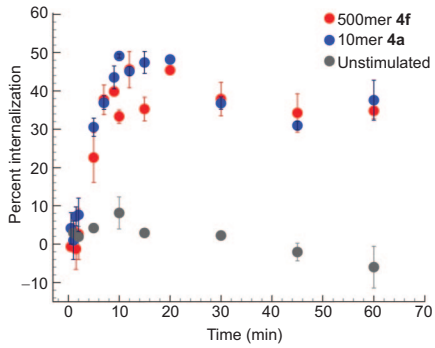

Figure 5. Internalization of the BCR induced by multivalent antigens. Washed A20/2J HL_{TNP} cells were incubated with antigen (4f or 4a or buffer control) and then incubated at either 4 or 37 °C for varying intervals of time. Cells were stained with Cy5-labeled F(ab′) fragment anti-IgM and analyzed by flow cytometry. Percent internalization was determined by dividing the geometric mean fluorescence intensity of the 37 °C sample by the geometric mean fluorescence intensity of the 4 °C sample and multiplying by 100.

min (DNP–BSA) at 4 or 37 °C and internalization was monitored by flow cytometric analysis using the aforementioned F(ab′). Treatment with DNP–BSA promoted significant levels of BCR internalization (data not shown). The addition of multivalent antigen **4a** or **4f**, resulted in similar amounts of BCR internalization (Figure 5). Thus, the differences observed in signals elicited by the multivalent ligands **4a** and **4f** do not appear to arise from differences in BCR internalization. These results provide evidence that BCR internalization and signaling are distinct.

BCR Clustering Induced by Multivalent Ligands. The differing abilities of the various multivalent ligands to promote BCR signaling might arise from their differing abilities to mediate BCR clustering. We employed fluorescence microscopy to ascertain whether such differences would be manifested. To label the DNP-specific BCRs without engaging multiple receptors, we used a monovalent Cy3-conjugated anti-IgM F(ab′) fragment. Before treatment of cells with multivalent ligands, this BCR marker exhibited diffuse staining across the cell surface (Figure 6, panel a). When cells were treated with anti-IgM $F(ab')_2$, which can induce BCR clustering, the receptor was localized to large patches (Figure 6, panel b). Similarly, we found that both the low valency (10mer **4a**) and high valency (500mer **4f**) DNP-substituted multivalent ligands induced clustering of the BCR (Figure 6, panels c and d). Although all synthetic ligands were capable of clustering the BCR, a higher degree of clustering was observed in cells treated with 500mer **4f** *versus* those treated with 10mer **4a**. Analysis of the images demonstrated that the spot size (number of pixels) increases, while the number of spots decreases when cells are treated with multivalent ligand (Figure 7). This analysis also indicates that the extent of clustering induced by 500mer **4f** is greater than that induced by 10mer **4a**. Many small BCR patches are seen on cells treated with 10mer **4a**; when cells are treated with 500mer **4f**, we observed fewer but much larger patches of BCR clusters (Figure 7). Thus, the increased signaling observed for the higher valency ligands may result from their ability to cluster the BCR.

This examination of BCR clustering highlights the differences in antibody-promoted *versus* multivalent antigen-induced BCR clustering. It is well established that anti-BCR antibodies promote clustering by the binding of multiple antibodies to multiple copies of the BCR (*i.e.*, two antibodies can bind a single BCR, and one antibody is capable of binding two BCRs, thus forming a large patch of BCRs bound by several antibodies, Figure 6, panel b). Intriguingly, the data indicate that the polymeric antigens do not act in a similar manner. If the polymers cluster the BCR using the same mechanism as the antibodies, each polymeric antigen should induce the same extent of clustering, regardless of valency. Our data indicate, however, that the extent of clustering and the magnitude of the Ca^{2+} flux depend on antigen valency (Figures 6, panels c and d, and 7). The ability of the polymeric antigens to induce clustering of the BCR to different extents likely stems from the inability of two polymer molecules to bind to a single BCR. Such a binding mode should be inhibited because of steric stabilization (*3*, *61*). Moreover, only those ligands that most effectively cluster the BCR elicit antibody production. These data emphasize the benefits of using polyvalent antigens over antibodies to explore BCR signaling.

Recruitment of the BCR to GM1-Rich Regions of the Membrane Depends on Ligand Valency. BCR clustering leads to its colocalization with glycosphingolipids such as GM1. This localization is often suggested to result from lipid microdomains. The existence and role of these domains are controversial (*62–64*), and recent data suggest that signaling proteins are localized

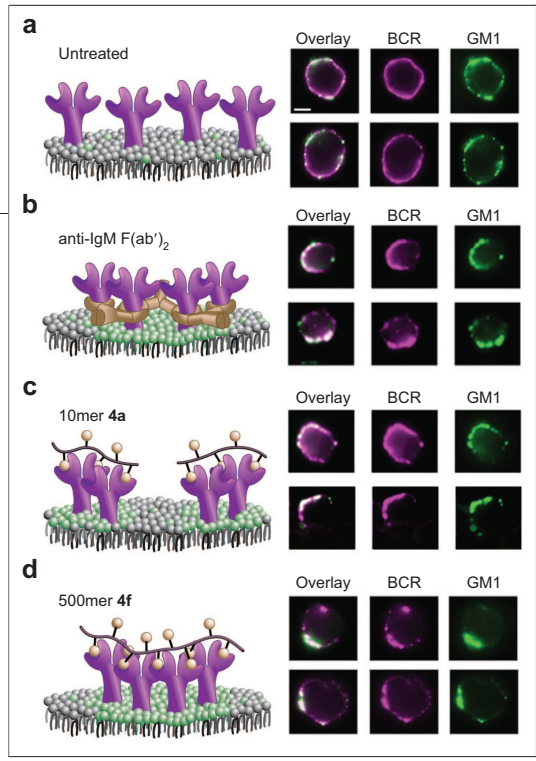

Figure 6. Visualization of BCR and GM1 localization on A20/2J HL_{TNP} cells treated with multivalent ligands. BCR (purple) was labeled with Cy3-conjugated anti-IgM F(ab′) and GM1 (green) was labeled with fluorescein-conjugated cholera toxin B-subunit. Overlays were constructed by combining images for BCR and GM1 using Adobe Photoshop. Scale bar equals 10 μm.

via protein–protein interactions (*65*). Whatever the role of these domains (*13, 60, 66–70*), multivalent antigens can promote BCR recruitment to GM1-rich regions. We therefore tested the influence of multivalent ligand valency on this localization. To identify GM1-rich regions, we employed fluorescein-labeled cholera toxin B-subunit, which recognizes GM1 on the plasma membrane. This tool, in conjunction with the Cy3-conjugated anti-IgM F(ab′) antibody mentioned above, provided the means to monitor recruitment of the BCR to GM1-rich regions.

Prior to treatment with either a BCR-cross-linking antibody or a multivalent antigen, cells labeled with fluorescein-conjugated cholera toxin B-subunit exhibited diffuse staining (Figure 6, panel a). Thus, GM1 is diffusely distributed on untreated cells. When cells are exposed to the anti-IgM $F(ab')_2$ antibody, however, large patches of GM1 are apparent that coincide with the clusters of BCRs. To explore the effects of the multivalent ligands, A20/2J HL_{TNP} cells were exposed to the DNP-substituted multivalent ligands (10mer **4a** and 500mer **4f**). The low valency antigen, 10mer **4a**, caused small clusters (though large in number) of BCR colocalized with GM1-enriched regions (Figure 6, panel c). In contrast, the 500mer **4f** induced clustering of BCR and its colocalization with GM1-enriched membrane regions (Figure 6, panel d). The resulting large patches overlap with GM1-enriched membrane regions. These observations, in conjunction with the signaling data, indicate that BCR clustering results in changes in membrane organization. The extent of a ligand's ability to induce BCR clustering and localization is related to its ability to elicit robust calcium signals.

Clustering of Unligated BCR Suggests Mechanism for Signal Amplification. The importance of receptor localization in BCR signaling led us to hypothesize that BCR signals might be amplified *via* receptor–receptor contacts. Other processes that depend upon signal amplification, including bacterial chemotaxis (*1, 71–73*), employ receptor–receptor interactions for amplifying signals. Experiments focused on elucidating how the T cell receptor (TCR) amplifies signals suggest that endogenous peptides bound to major histocompatibility complexes (MHCs) contribute to T cell activation (*74*). These data suggest that TCRs not bound to antigenic peptides contribute to activation. The use of receptor–receptor interactions for amplifying signals initiated through the BCR is attractive, because this receptor must respond with high sensitivity to physiological signals.

The finding that receptor–receptor contacts contribute to signal amplification in *Escherichia coli* is supported by data indicating that unliganded chemoreceptors cluster with bound receptors (*6*). We reasoned that if receptor–receptor contacts are important for BCR signaling, unliganded BCRs would cocluster with liganded receptors. To test for such colocalization, we took advantage of the presence of a BCR of IgG subtype (with unknown specificity) on the A20/2J HL_{TNP} cell surface.

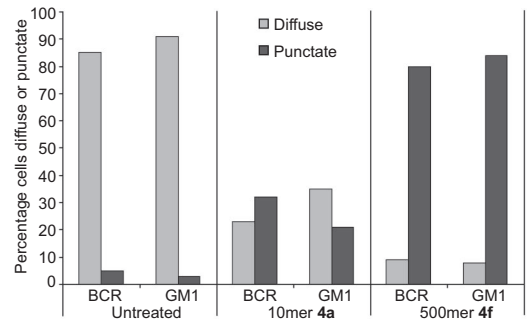

Figure 7. Graph depicting the percentages of cells exhibiting diffuse or punctate staining after multivalent antigen treatment. The percentages were devised from statistical analysis of images of cells treated with buffer (control), 10mer 4a, or 500mer 4f DNP-substituted homopolymers. For each sample, several fields were randomly selected and 50–100 cells total were analyzed per treatment. Diffuse *vs* punctate staining was scored. Some cells exhibited inconclusive staining that could not be assigned as diffuse or punctate. The results are a composite from analysis of cells from three independent experiments.

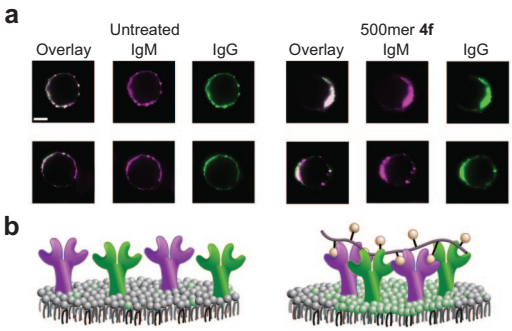

Figure 8. Visualization of unliganded BCR, liganded BCR, and GM1 localization on A20/2J HL_{TNP} cells treated with multivalent ligand 4f. In panel a, the DNP-specific BCR (IgM; purple) was labeled with fluorescein-conjugated anti-IgM F(ab′) and the unliganded BCR (IgG; green) was stained with Cy3-conjugated anti-IgG F(ab′). The model in panel b depicts unliganded BCR (green; IgG) colocalizing with BCRs engaged and clustered by our multivalent antigen (purple; IgM). Overlays were constructed by combining images for BCR and GM1 using Adobe Photoshop. Scale bar equals 10 μm.

Each BCR subtype could be visualized independently. Interestingly, our data indicate that these subtypes colocalize in untreated cells (Figure 8, panel a). This finding is consistent with other results that indicate BCRs interact to form an extended array. To ascertain whether unligated receptors interact with ligated receptors, we envisioned clustering the DNP-specific BCR (IgM subtype) with the multivalent antigens and determining the localization of the unliganded BCR (IgG subtype). Our data indicate that the BCR of IgG subtype does not interact with the multivalent ligands; no signaling was observed when A20 cells (which only display this IgG-subtype BCR) were treated with the multivalent ligands. Accordingly, we exposed A20/2J HL_{TNP} cells to the DNP-presenting multivalent 500mer **4f** and monitored localization of each BCR subtype. Intriguingly, treatment with the 500mer at low temperatures afforded large patches that contain unligated BCR (IgG). These patches overlap with the DNP-specific BCR (IgM subtype) (Figure 8). These data suggest that unliganded BCRs colocalize with the liganded BCRs that are responsible for signal transmission. They are consistent with models in which BCR arrays mediate antigen sensing (*75*). Indeed, our data implicate a role for BCR–BCR interactions in signal amplification.

CONCLUSION

The multivalent ligands we have generated can dissect the inter-relationships between BCR clustering, localization, internalization, and signal amplification. Our results indicate that the extent of signaling, degree of BCR clustering, and antibody production are all influenced profoundly by antigen valency. In contrast, the extent of BCR internalization is not correlated with antigen valency, a result that suggests that BCR signaling and internalization are distinct processes. Our data highlight the ability of the multivalent ligands generated by ROMP to systematically probe signaling, not only *in vitro* but also *in vivo*. Thus, they underscore the value and versatility of these polymers as biological probes.

Our data support models in which clustering of BCRs is required for antigen-dependent signaling. In addition to the clustering of ligand-bound BCRs, unbound receptors are also clustered, a result that suggests they contribute to signal amplification. Indeed, the data are consistent with a model in which BCR signals are amplified through receptor arrays. Because B cells must respond with high sensitivity, these arrays can provide the means through which B cells transmit antigen signals into outcomes that range from immunity to tolerance.

EXPERIMENTAL PROCEDURES

Generation of Multivalent Ligands for Investigating B Cell Signaling. Solvents and reagents were obtained from commercial suppliers. Dichloromethane (DCM) was distilled from calcium hydride, cooled to −78 °C under high vacuum, and kept under N_2. Gastight syringes were dried in a drying piston. Analytical thin-layer chromatography (TLC) was performed on 0.25 mm precoated Merck Silica Gel 60 F_{254}, and compounds were visualized with potassium permanganate stain. Disposable PD-10 (Sephadex G25-resin) size exclusion columns were obtained from Amersham Biosciences. All gel permeation chromatography (GPC) analysis was done with equipment obtained from Polymer Laboratories. EasiCal Polystyrene Standards MW 580–7,500,000 were used to make a calibration curve. Polymer analysis was done by injection of 100 μL of samples in 1 mg mL^{-1} tetrahydrofuran into two PLgel 5 μm MIXED-D 300 × 7.5 mm columns connected in series. Cirrus GPC Software was employed in data analysis.

Synthesis of Succinimidyl Ester-Containing Polymer **3a**. To a solution of monomer **1** (100.0 mg, 0.4251 mmol, 10 equiv) in deoxygenated DCM was added a solution of ruthenium initiator **2** (37.6 mg, 0.0425 mmol, 1 equiv) in deoxygenated DCM such that the monomer concentration of the resulting solution was 0.1 M. The resulting purple solution was stirred at −20 °C for 45 min until analysis by TLC showed no remaining monomer. Excess ethyl vinyl ether (1 drop) was added to terminate the polymerization. After 3 h,

the polymer was precipitated in a vortexing solution of 9:1 ether/benzene (60 mL). The solution was centrifuged and decanted, and the solid was dried to provide polymer **3a** (M:I 10:1, 89.7 mg, 83%) as a granular gray solid.

Synthesis of DNP-Substituted Polymer. To polymer **3a** (0.9 mg, 3.8 μmol, 1 equiv) in an Eppendorf tube was added a solution of 2,4-dinitrophenyllysine·HCl in DMSO (39.2 μL). *N*-Methylmorpholine (2.1 μL, 19.1 μmol, 5 equiv) was added. After 24 h, ethanolamine (1.2 μL, 19.1 μmol, 5 equiv) was added to convert excess succinimidyl ester groups to neutral functionality, thereby generating **4a**–**f**. After 24 h, polymers were purified by a PD-10 (Sephadex G-25 resin) size exclusion column using water as an eluent. The water was removed using speed vacuum concentration. ^{1}H-NMR in d_6-DMSO was employed to determine a mole fraction (χ) of DNP substitution (0.4) on the final multivalent antigen (1.0 mg, 93% yield).

Anti-DNP IgM Production and Detection. Female BALB/c mice, 6–8 weeks old, were injected with 0 (control), 0.01, 0.1, 1, or 10 ng of either 10mer **4a** or 500mer **4f** suspended in Dulbecco's phosphate-buffered saline (DPBS; Invitrogen)/complete Freund's adjuvant (CFA; Sigma) emulsion. Postinjection 6–15 d, serum was isolated from the animals and was screened for DNP-specific IgM. To assess production of the desired antibodies, an ELISA was performed. Polysorb plates (96-well) were first coated overnight at 4 °C with 1 μg mL^{-1} DNP-(*30*)-BSA (DNP-conjugated BSA). After three washes with DPBS, plates were blocked with Superblock T20 PBS (Pierce) for 1 h at RT, and were then washed extensively with DPBS. Wells were then incubated for 1 h at RT with dilutions of antibody serum isolated from the injected animals. Serum dilutions were made using Superblock T20. After additional DPBS washes, wells were incubated with horseradish peroxidase-conjugated goat anti-mouse-IgM for 1 h at RT. Wells were then incubated with substrate TMB 1-step turbo (Pierce) and were quenched with 1 N H_2SO_4, and plates were read at 450 nm. Animal studies were performed in accordance with the University of Wisconsin–Madison Research Animal Resources Center, which adheres to both national and local guidelines and regulations for proper care and usage of research animals.

Cell Culture and Media. A20/2J cells stably transfected with heavy and light chains for DNP/TNP-specific mIgM, termed A20/2J HL$_{TNP}$ (*16*), were cultured in Roswell Park Memorial Institute medium (RPMI) 1640 media supplemented with 2 mM L-glutamine, 10% fetal bovine serum (FBS), 50 μM β-mercaptoethanol, 100 U mL^{-1} penicillin, and 100 U mL^{-1} streptomycin. For cell culture and experimentation, cells were stripped from adherent flasks by incubation at 37 °C in DPBS pH 7.1 containing 1 mM EDTA (Sigma) for 10 min. A20 cells were cultured in RPMI 1640 supplemented with 2 mM L-glutamine, 10% FBS, 100 μM β-mercaptoethanol, 100 U mL^{-1} penicillin, and 100 U mL^{-1} streptomycin.

Multivalent Ligand Signaling through the BCR Monitored by Ca^{2+} Flux. Cells (2×10^6 cells mL^{-1}) were washed extensively in DPBS (pH 7.1) loaded with 6 μg mL^{-1} indo-1, AM (Molecular Probes), for 40 min at 37 °C. Loaded cells were then washed in calcium flux buffer and DBPS supplemented with 1% BSA and 1 mM $CaCl_2$ and diluted to 1×10^6 cells mL^{-1}. Indo-1 loaded cells were analyzed using a Becton-Dickinson fluorescence-activated cell sorting (FACS)-Diva flow cytometer and the fluorescence ratio (R) was monitored as F_2/F_1, where F_2 corresponds to emission from Ca^{2+}-bound indo-1 (~405 nm) and F_1 represents emission from Ca^{2+}-free indo-1 (~490 nm). After collection of baseline emission for 40 s, cells were stimulated with multivalent ligand or antibody control (F(ab′)$_2$ anti-IgM fragment was used because it can bind and cluster the BCR without engaging inhibitory Fc receptors). The indo-1 emission ratio was recorded for 260 s after stimulation. $[Ca^{2+}]_i$ was determined using the formula $[Ca^{2+}]_i = K_d B[(R - R_{min})/(R_{max} - R)]$, where K_d is the dissociation constant for indo-1 and Ca^{2+} and $B = F_{1,min}/F_{1,max}$ (*76, 77*). Minimum and maximum values for R and F_1 were determined by analysis of cells in Ca^{2+}-free solution (DPBS pH 7.1 with 3 mM EGTA) and at saturating levels of Ca^{2+} (cells treated with 5 μM ionomycin in calcium flux buffer), respectively. Data analysis was performed using the FlowJo kinetics platform.

BCR Internalization. A20/2J HL$_{TNP}$ cells were harvested, washed twice with FACS buffer, and resuspended to a concentration of 2×10^6 viable cells mL^{-1}. The cells were incubated with antigen (polymer, DNP–BSA, or buffer control) for 60 min at 4 °C and then pelleted to remove unbound ligands. The cell pellets were resuspended in FACS buffer to the original concentration of 2×10^6 viable cells mL^{-1}. Half of the sample was then warmed to 37 °C for a specific time period. The second half of the sample remained at 4 °C. After the relevant incubation time, the cells were stained with Cy5-labeled Fab fragment anti-IgM for 30 min at 4 °C, washed twice, and resuspended in FACS buffer for analysis by flow cytometry. The percent internalization was calculated by dividing the geometric mean fluorescence intensity of the 37 °C sample by the geometric mean fluorescence intensity of the 4 °C sample and multiplying by 100.

BCR Clustering and Lipid Microdomain Corecruitment. Cells (5×10^6 cells mL^{-1}) were washed extensively in binding buffer, DPBS pH 7.1 supplemented with 1% BSA (Research Organics). To examine localization of the DNP-specific BCR and GM1, cells were stained for 30 min on ice, with 16 μg mL^{-1} Cy3-conjugated anti-IgM μ-chain F(ab′) and 50 μg mL^{-1} fluorescein-conjugated Cholera toxin B-subunit (Figure 6). To monitor localization of unliganded BCRs (IgG) with respect to liganded BCRs (IgM) and lipid microdomains (GM1), cells were stained 16 μg mL^{-1} Cy3-conjugated and 16 μg mL^{-1} fluorescein-conjugated anti-IgM μ-chain F(ab′) (Figure 7, panel a), or 16 μg mL^{-1} Cy3-conjugated anti-IgG F(ab') and 50 μg mL^{-1} fluorescein-conjugated Cholera toxin B-subunit (Figure 7, panel b) for 30 min on ice. After being washed extensively with binding buffer, stained cells were incubated with compounds **4a** or **4f** or with anti-IgM F(ab′)$_2$ for 10 min on ice. The cells were then washed twice with DPBS and then fixed with 4% *p*-formaldehyde for 30 min on ice. After additional washing with binding buffer, cells were mounted on polylysine-coated slides and analyzed with a Nikkon E800 microscope and MetaMorph software (Universal Imaging Co., Downing, PA). For each slide, several fields were randomly selected on bright field, and 50–100 cells were analyzed per slide. Roughly 10% of the stained cells exhibited either weak staining or very high/nonspecific staining; these cells were omitted from analysis. Of the remaining cells, diffuse *versus* bright, punctate staining was scored.

Acknowledgment: This research was supported by the National Institutes of Health (AI055258). E.B.P. is the recipient of a Steenbock predoctoral fellowship and J.J.H. was supported by an NIH postdoctoral fellowship (AI054092). We thank the University of Wisconsin Comprehensive Cancer Center Flow Cytometry Facility for their technical assistance and C. Wiese for the use of equipment. The A20.2J HL/TNP cell line was a generous gift of A. Ochi.

Competing Interests Statement: The authors declare that they have no competing financial interests.

REFERENCES

1. Kiessling, L. L., Gestwicki, J. E., and Strong, L. E. (2006) Synthetic multivalent ligands as probes of signal transduction, *Angew. Chem., Int. Ed. 45*, 2348–2368.
2. Kiessling, L. L., Gestwicki, J. E., and Strong, L. E. (2000) Synthetic multivalent ligands in the exploration of cell-surface interactions, *Curr. Opin. Chem. Biol. 4*, 696–703.

3. Mammen, M., Choi, S.-K., and Whitesides, G. M. (1998) Polyvalent interactions in biological systems: implications for design and use of multivalent ligands and inhibitors, *Angew. Chem., Int. Ed. 37*, 2754–2794.
4. Heldin, C. H. (1995) Dimerization of cell surface receptors in signal transduction, *Cell 80*, 213–223.
5. Klemm, J. D., Schreiber, S. L., and Crabtree, G. R. (1998) Dimerization as a regulatory mechanism in signal transduction, *Annu. Rev. Immunol. 16*, 569–592.
6. Gestwicki, J. E., and Kiessling, L. L. (2002) Inter-receptor communication through arrays of bacterial chemoreceptors, *Nature 415*, 81–84.
7. Gestwicki, J. E., Strong, L. E., Borchardt, S. L., Cairo, C. W., Schnoes, A. M., and Kiessling, L. L. (2001) Designed potent multivalent chemoattractants for Escherichia coli, *Bioorg. Med. Chem. 9*, 2387–2393.
8. Lamanna, A. C., Gestwicki, J. E., Strong, L. E., Borchardt, S. L., Owen, R. M., and Kiessling, L. L. (2002) Conserved amplification of chemotactic responses through chemoreceptor interactions, *J. Bacteriol. 184*, 4981–4987.
9. Goodnow, C. C. (1996) Balancing immunity and tolerance: deleting and tuning lymphocyte repertoires, *Proc. Natl. Acad. Sci. U.S.A. 93*, 2264–2271.
10. Goldsby, R. A., Kindt, T. J., and Osborne, B. A. (2000) *Immunology (Kuby)*, 4th ed., W.H. Freeman and Co., New York.
11. Healy, J. I., and Goodnow, C. C. (1998) Positive versus negative signaling by lymphocyte antigen receptors, *Annu. Rev. Immunol. 16*, 645–670.
12. Niiro, H., and Clark, E. A. (2002) Regulation of B-cell fate by antigen-receptor signals, *Nat. Rev. Immunol. 2*, 945–956.
13. Thyagarajan, R., Arunkumar, N., and Song, W. (2003) Polyvalent antigens stabilize B cell antigen receptor surface signaling microdomains, *J. Immunol. 170*, 6099–6106.
14. Hokazono, Y., Adachi, T., Wabl, M., Tada, N., Amagasa, T., and Tsubata, T. (2003) Inhibitory coreceptors activated by antigens but not by anti-Ig heavy chain antibodies install requirement of costimulation through CD40 for survival and proliferation of B cells, *J. Immunol. 171*, 1835–1843.
15. Cherukuri, A., Cheng, P. C., Sohn, H. W., and Pierce, S. K. (2001) The CD19/21 complex functions to prolong B cell antigen receptor signaling from lipid rafts, *Immunity 14*, 169–179.
16. Sato, K., and Ochi, A. (1998) Inhibition of B-cell receptor-antigen complex internalization by FcγRIIB1 signals, *Immunol. Lett. 61*, 135–143.
17. Cairo, C. W., Gestwicki, J. E., Kanai, M., and Kiessling, L. L. (2002) Control of multivalent interactions by binding epitope density, *J. Am. Chem. Soc. 124*, 1615–1619.
18. Desaymard, C., and Howard, J. G. (1975) Role of epitope density in the induction of immunity and tolerance with thymus-independent antigens. II, *Eur. J. Immunol. 5*, 541–545.
19. Desaymard, C., and Feldmann, M. (1975) Role of epitope density in the induction of immunity and tolerance with thymus-independent antigens. I. Studies with 2,4-dinitrophenyl conjugates in vitro, *Eur. J. Immunol. 5*, 537–541.
20. Dintzis, H. M., Dintzis, R. Z., and Vogelstein, B. (1976) Molecular determinants of immunogenicity: the immunon model of immune response, *Proc. Natl. Acad. Sci. U.S.A. 73*, 3671–3675.
21. Dintzis, R. Z., Vogelstein, B., and Dintzis, H. M. (1982) Specific cellular stimulation in the primary immune response: experimental test of a quantitized model, *Proc. Natl. Acad. Sci. U.S.A. 79*, 884–888.
22. Dintzis, R. Z., Okajima, M., Middleton, M. H., Greene, G., and Dintzis, H. M. (1989) The immunogenicity of soluble haptenated polymers is determined by molecular mass and hapten valency, *J. Immunol. 143*, 1239–1244.
23. Choi, T.-L., and Grubbs, R. H. (2003) Controlled living ring-opening-metathesis polymerization by a fast-initiating ruthenium catalyst, *Angew. Chem., Int. Ed. 42*, 1743–1746.
24. Lynn, D. M., Kanaoka, S., and Grubbs, R. H. (1996) Living ring-opening metathesis polymerization in aqueous media catalyzed by well-defined ruthenium carbene complexes, *J. Am. Chem. Soc. 118*, 784–790.
25. Pontrello, J. K., Allen, M. J., Underbakke, E. S., and Kiessling, L. L. (2005) Solid-phase synthesis of polymers using the ring-opening metathesis polymerization, *J. Am. Chem. Soc. 127*, 14536–14537.
26. Allen, M. J., Raines, R. T., and Kiessling, L. L. (2006) Contrast agents for magnetic resonance imaging synthesized with ring-opening metathesis polymerization, *J. Am. Chem. Soc. 128*, 6534–6535.
27. Schwab, P., Grubbs, R. H., and Ziller, J. W. (1996) Synthesis and applications of $RuCl_2(CHR')(PR_3)$ 2: the influence of the alkylidene moiety on metathesis activity, *J. Am. Chem. Soc. 118*, 100–110.
28. Lee, Y., and Sampson, N. S. (2006) Romping the cellular landscape: linear scaffolds for molecular recognition, *Curr. Opin. Struct. Biol. 16*, 544–550.
29. Gestwicki, J. E., Strong, L. E., and Kiessling, L. L. (2000) Tuning chemotactic responses using synthetic multivalent ligands, *Chem. Biol. 7*, 583–591.
30. Gordon, E. J., Sanders, W. J., and Kiessling, L. L. (1998) Synthetic ligands point to cell surface strategies, *Nature 392*, 30–31.
31. Gordon, E. J., Strong, L. E., and Kiessling, L. L. (1998) Glycoprotein-inspired materials promote the proteolytic release of cell surface L-selectin, *Bioorg. Med. Chem. 6*, 1293–1299.
32. Kiessling, L. L., and Gordon, E. J. (1998) Transforming the cell surface through proteolysis, *Chem. Biol. 5*, R49–62.
33. Mowery, P., Yang, Z. Q., Gordon, E. J., Dwir, O., Spencer, A. G., Alon, R., and Kiessling, L. L. (2004) Synthetic glycoprotein mimics inhibit L-selectin-mediated rolling and promote L-selectin shedding, *Chem. Biol. 11*, 725–732.
34. Sanders, W. J., Gordon, E. J., Dwir, O., Beck, P. J., Alon, R., and Kiessling, L. L. (1999) Inhibition of L-selectin-mediated leukocyte rolling by synthetic glycoprotein mimics, *J. Biol. Chem. 274*, 5271–5278.
35. Strong, L. E., and Kiessling, L. L. (1999) A general synthetic route to defined, biologically active multivalent arrays, *J. Am. Chem. Soc. 121*, 6193–6196.
36. Manning, D. D., Strong, L. E., Xin, H., Beck, P. J., and Kiessling, L. L. (1997) Neoglycopolymer inhibitors of the selectins, *Tetrahedron 53*, 11937–11952.
37. Love, J. A., Morgan, J. P., Trnka, T. M., and Grubbs, R. H. (2002) A practical and highly active ruthenium-based catalyst that effects the cross metathesis of acrylonitrile, *Angew. Chem., Int. Ed. 41*, 4035–4037.
38. Barrett, A. G. M., Hopkins, B. T., and Kobberling, J. (2002) ROMPgel reagents in parallel synthesis, *Chem. Rev. 102*, 3301–3324.
39. Tolar, P., Sohn, H. W., and Pierce, S. K. (2005) The initiation of antigen-induced B cell antigen receptor signaling viewed in living cells by fluorescence resonance energy transfer, *Nat. Immunol. 6*, 1168–1176.
40. Kanai, M., Mortell, K. H., and Kiessling, L. L. (1997) Varying the size of multivalent ligands: the dependence of concanavalin A binding on neoglycopolymer length, *J. Am. Chem. Soc. 119*, 9931–9932.
41. Mann, D. A., Kanai, M., Maly, D. J., and Kiessling, L. L. (1998) Probing low affinity and multivalent interactions with surface plasmon resonance: ligands for concanavalin A, *J. Am. Chem. Soc. 120*, 10575–10582.
42. Gestwicki, J. E., Cairo, C. W., Strong, L. E., Oetjen, K. A., and Kiessling, L. L. (2002) Influencing receptor-ligand binding mechanisms with multivalent ligand architecture, *J. Am. Chem. Soc. 124*, 14922–14933.
43. Szmacinski, H., Gryczynski, I., and Lakowicz, J. R. (1993) Calcium-dependent fluorescence lifetimes of Indo-1 for one- and two-photon excitation of fluorescence, *Photochem. Photobiol. 58*, 341–345.

44. Trischmann, U., Klockner, U., Isenberg, G., Utz, J., and Ullrich, V. (1991) Carbon monoxide inhibits depolarization-induced Ca rise and increases cyclic GMP in visceral smooth muscle cells, *Biochem. Pharmacol. 41*, 237–241.
45. Kim, Y. M., Pan, J. Y., Korbel, G. A., Peperzak, V., Boes, M., and Ploegh, H. L. (2006) Monovalent ligation of the B cell receptor induces receptor activation but fails to promote antigen presentation, *Proc. Natl. Acad. Sci. U.S.A. 103*, 3327–3332.
46. Dintzis, R. Z., Middleton, M. H., and Dintzis, H. M. (1983) Studies on the immunogenicity and tolerogenicity of T-independent antigens, *J. Immunol. 131*, 2196–2203.
47. Sulzer, B., and Perelson, A. S. (1997) Immunons revisited: binding of multivalent antigens to B cells, *Mol. Immunol. 34*, 63–74.
48. Griffith, B. R., Allen, B. L., Rapraeger, A. C., and Kiessling, L. L. (2004) A polymer scaffold for protein oligomerization, *J. Am. Chem. Soc. 126*, 1608–1609.
49. Goodnow, C. C. (1992) Transgenic mice and analysis of B-cell tolerance, *Annu. Rev. Immunol. 10*, 489–518.
50. Dolmetsch, R. E., Lewis, R. S., Goodnow, C. C., and Healy, J. I. (1997) Differential activation of transcription factors induced by Ca^{2+} response amplitude and duration, *Nature 386*, 855–858.
51. Diner, U. E., Kunimoto, D., and Diener, E. (1979) Carboxymethyl cellulose, a nonimmunogenic hapten carrier with tolerogenic properties, *J. Immunol. 122*, 1886–1891.
52. Dintzis, H. M., and Dintzis, R. Z. (1990) Antigens as immunoregulators. *Immunol. Rev. 115*, 243–250; discussion 251.
53. Dintzis, H. M., and Dintzis, R. Z. (1992) Profound specific suppression by antigen of persistent IgM, IgG, and IgE antibody production, *Proc. Natl. Acad. Sci. U.S.A. 89*, 1113–1117.
54. Reim, J. W., Symer, D. E., Watson, D. C., Dintzis, R. Z., and Dintzis, H. M. (1996) Low molecular weight antigen arrays delete high affinity memory B cells without affecting specific T-cell help, *Mol. Immunol. 33*, 1377–1388.
55. Jones, D. S. (2005) Multivalent compounds for antigen-specific B cell tolerance and treatment of autoimmune diseases, *Curr. Med. Chem. 12*, 1887–1904.
56. Matyjaszewski, K., and Xia, J. (2001) Atom transfer radical polymerization, *Chem. Rev. 101*, 2921–2990.
57. Schrock, R. R. (1990) Living ring-opening metathesis polymerization catalyzed by well-characterized transition-metal alkylidene complexes, *Acc. Chem. Res. 23*, 158–165.
58. Webster, O. W. (1991) Living polymerization methods, *Science 251*, 887–893.
59. Hou, P., Araujo, E., Zhao, T., Zhang, M., Massenburg, D., Veselits, M., Doyle, C., Dinner, A. R., and Clark, M. R. (2006) B Cell antigen receptor signaling and internalization are mutually exclusive events, *PLoS Biol. 4*, 1147–1158.
60. Stoddart, A., Jackson, A. P., and Brodsky, F. M. (2005) Plasticity of B cell receptor internalization upon conditional depletion of clathrin, *Mol. Biol. Cell. 16*, 2339–2348.
61. Yang, J., Mayer, M., Kriebel, J. K., Garstecki, P., and Whitesides, G. M. (2004) Self-assembled aggregates of IgGs as templates for the growth of clusters of gold nanoparticles, *Angew. Chem., Int. Ed. 43*, 1555–1558.
62. Hancock, J. F. (2006) Lipid rafts: contentious only from simplistic standpoints, *Nat. Rev. Mol. Cell Biol. 7*, 456–462.
63. Nichols, B. (2005) Without a raft, *Nature 436*, 638–639.
64. Shaw, A. S. (2006) Lipid rafts: now you see them, now you don't, *Nat. Immunol. 7*, 1139–1142.
65. Douglass, A. D., and Vale, R. D. (2005) Single-molecule microscopy reveals plasma membrane microdomains created by protein–protein networks that exclude or trap signaling molecules in T cells, *Cell 121*, 937–950.
66. Cheng, P. C., Brown, B. K., Song, W., and Pierce, S. K. (2001) Translocation of the B cell antigen receptor into lipid rafts reveals a novel step in signaling, *J. Immunol. 166*, 3693–3701.
67. Cheng, P. C., Cherukuri, A., Dykstra, M., Malapati, S., Sproul, T., Chen, M. R., and Pierce, S. K. (2001) Floating the raft hypothesis: the roles of lipid rafts in B cell antigen receptor function, *Semin. Immunol. 13*, 107–114.
68. Dykstra, M., Cherukuri, A., Sohn, H. W., Tzeng, S. J., and Pierce, S. K. (2003) Location is everything: lipid rafts and immune cell signaling, *Annu. Rev. Immunol. 21*, 457–481.
69. Pierce, S. K. (2002) Lipid rafts and B-cell activation, *Nat. Rev. Immunol. 2*, 96–105.
70. Zacharias, D. A., Violin, J. D., Newton, A. C., and Tsien, R. Y. (2002) Partitioning of lipid-modified monomeric GFPs into membrane microdomains of live cells, *Science 296*, 913–916.
71. Bray, D. (1998) Signaling complexes: biophysical constraints on intracellular communication, *Annu. Rev. Biophys. Biomol. Struct. 27*, 59–75.
72. Reth, M., and Wienands, J. (1997) Initiation and processing of signals from the B cell antigen receptor, *Annu. Rev. Immunol. 15*, 453–479.
73. Torres, R. M., Flaswinkel, H., Reth, M., and Rajewsky, K. (1996) Aberrant B cell development and immune response in mice with a compromised BCR complex, *Science 272*, 1804–1808.
74. Krogsgaard, M., Li, Q. J., Sumen, C., Huppa, J. B., Huse, M., and Davis, M. M. (2005) Agonist/endogenous peptide-MHC heterodimers drive T cell activation and sensitivity, *Nature 434*, 238–243.
75. Schamel, W. W., and Reth, M. (2000) Monomeric and oligomeric complexes of the B cell antigen receptor, *Immunity 13*, 5–14.
76. Grynkiewicz, G., Poenie, M., and Tsien, R. Y. (1985) A new generation of Ca^{2+} indicators with greatly improved fluorescence properties, *J. Biol. Chem. 260*, 3440–3450.
77. Tsien, R., and Pozzan, T. (1989) Measurement of cytosolic free Ca^{2+} with quin2, *Methods Enzymol. 172*, 230–262.